V
Experimental Results

In this section are shown all the experimental measurements carried out with the SPR spectrometer developed in the laboratory using a He-Ne laser with a wavelength of 632.8 nm. The experimental curves of R_A Vs θ_x were analyzed and elaborated using the software *Winspall* 3.02. First we determined the dielectric function of thin planar nanometric films of silver and gold together with its variations due non- homogeneity of the metals depositions. After we show how is possible to measure the dielectric function of a thin film of Alq_3 using the Two-Metal Substrate Method. Finally, we performed the real-time monitoring of the degradation process of the interface Au/Alq_3 when exposed to atmospheric environment.

V.1 Measurement of the optical constants of thin silver films

In order to measure the dielectric function of silver we deposited 48 nm of silver (99.99%) on three glass slides at a base pressure of 3.43×10^{-6}Torr and a deposition rate of 1.7 Å/s. To study the variation of dielectric function on the same deposition, 10 points were chosen on each sample and analyzed by SPR spectroscopy. The distance between the points was about 2 mm. SPR curves were measured with an angular resolution of 0.00025° and an uncertainty of 0.03° , which is basically the uncertainty of the 0 angle determination. In figure V.1 are shown the measurements obtained for three different points (A,B,C) on one of the fabricated samples.

The full width at half maximum (FWHW) of the curves is 0.59°. The variation in the resonance angle for the 10 different points was about ±0.004°, quite smaller than the uncertainty in the 0 angle determination. The data obtained were analyzed with *Winspall* in order to determine the dielectric function and thickness of the films. One of the fit obtained is shown in figure V.2: here the number of theoretical points (*pktanz*) used to generate the theoretical curve was 3500 and the maximum number of iterations was 500.

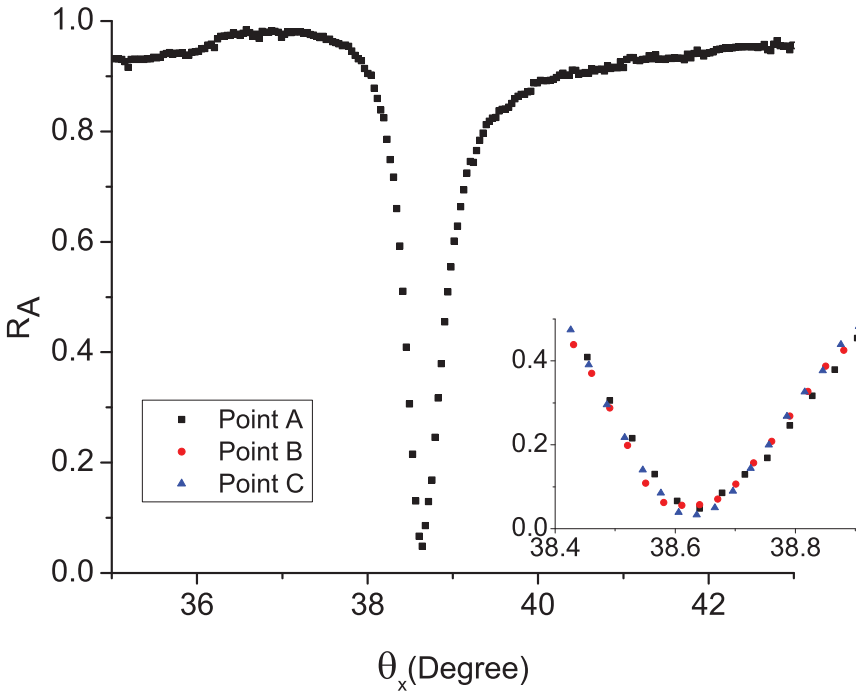

Figure V.1: Typical SPR curve for a silver deposition. The inserted figure represents the SPR curves, close to the ressonance angle, relative to three different points (A,B,C) on the same sample.

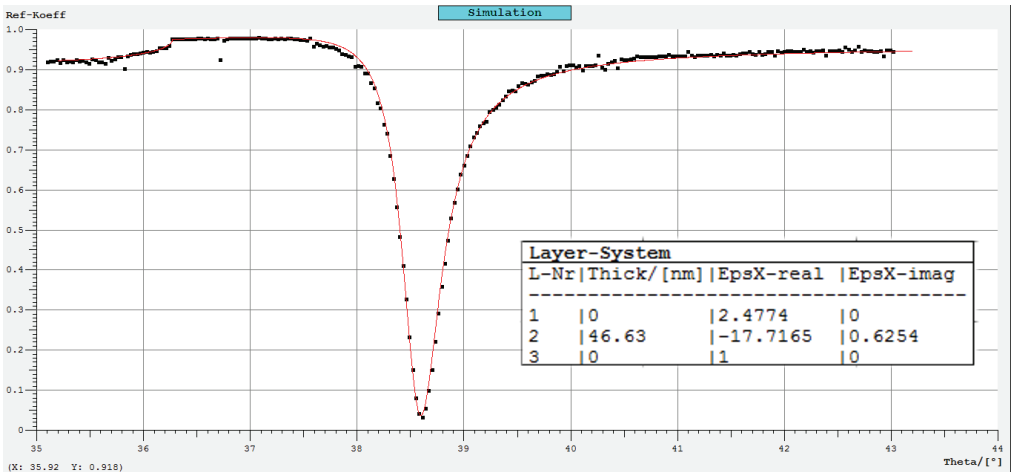

Figure V.2: Fit of the experimental SPR curve obtained with *Winspall* for one point over one of the silver thin films deposited. The black points represent the experimental measurements while the red curve is the theoretical one.

The values of thickness and index of refraction of the thin film deposition obtained by *Winspall* are summarized in table V.1.

The plasmon resonance angle (θ_{SPR}) is dependent on the thickness of the deposition and the real part of the dielectric function of the metal, whereas the imaginary part of the dielectric function together with the thickness of the layer influence the FWHW and the minimum value of the SPR curve.

	Thickness (nm)	ε_r	ε_{im}	θ_{SPR} (°)
Mean	46.3	-17.75	0.62	38.606
σ ±	0.3	0.06	0.02	0.004
% **Error**	0.6	0.3	3.2	x

Table V.1: Values obtained for thickness and dielectric function of one of the silver thin films fabricated. The uncertainty of the values reflects the non homogeneity of the metal deposition.

After performing the optical measurement we used the profilometer (see section III.2(b) for more information) to measure the thickness of the same silver film (fig. V.3) obtaining an average value of about (460±30)Å, consistent with the result obtained by SPR spectroscopy. The standard deviation (σ ±) indicated in table V.1 is essentially due the non homogeneity of the thin film deposition and is computed considering the dispersion of the values obtained performing the measurements on different parts of the sample. We put in evidence that the average experimental value of the dielectric function of silver at 632.8 nm is close to the ones reported in literature [Simon75][Bruijn90].

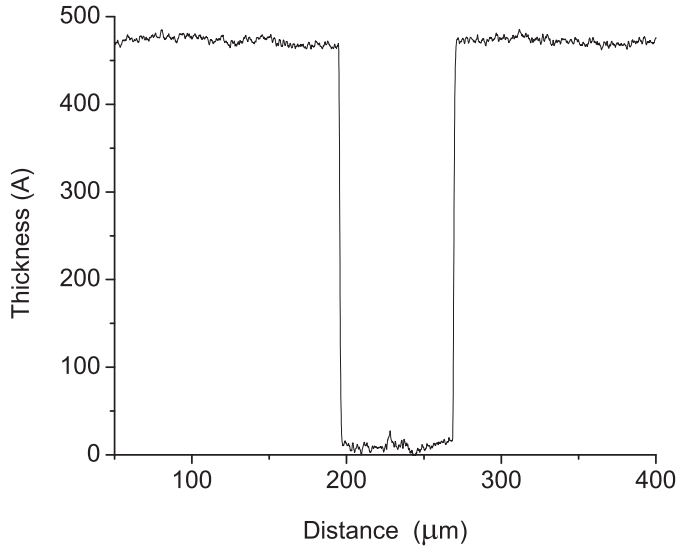

Figure V.3: One of the height profile relative to the the sample with the thin deposition of silver. The height profile has been obtained using the profilometer with a stylus force of 2mg and a scan length of 400 μm.

The measurement procedure described above was repeated for three different samples fabricated with the same metal deposition by e-Beam gun apparatus. The values of the dielectric function and the thickness of the metal over each film are summarized in table V.2

The dispersion of the optical constants of the different silver films is quite bigger than the dispersion obtained considering the non homogeneity of the

Sample	**Thickness** (nm)	ε_r	ε_{im}	θ_{SPR} (°)
1	46.3	-17.74	0.62	38.60
2	45.8	-17.59	0.65	38.63
3	44.8	-17.83	0.69	38.66

Table V.2: Values obtained for the dielectric function and thickness of different silver thin films fabricated during the same deposition by e-Beam gun apparatus.

silver deposition over one single sample. This is probably due the fact that the different samples were measured in different days. It is known that temperature affects the value of the optical constants of metals [Ozdemir03] and that a small layer of silver sulfide Ag_2S grows on the silver surface when exposed to air with a rate of about 1 nm per week [Bruijn90][McAneney09]. Silver samples were left in the vacuum chamber to minimize the formation of the Ag_2S layer, but is difficult to assure the complete preservation of the metal surface.

V.2 Measurement of the optical constants of thin gold films

Three gold films of 48 nm nominal thickness were deposited on glass slides by the e-Beam gun apparatus (pressure= 3.8×10^{-6} Torr, deposition rate 2 Å/s). The SPR curves relative to three different position (A,B,C) over the same gold sample are shown in figure V.4.

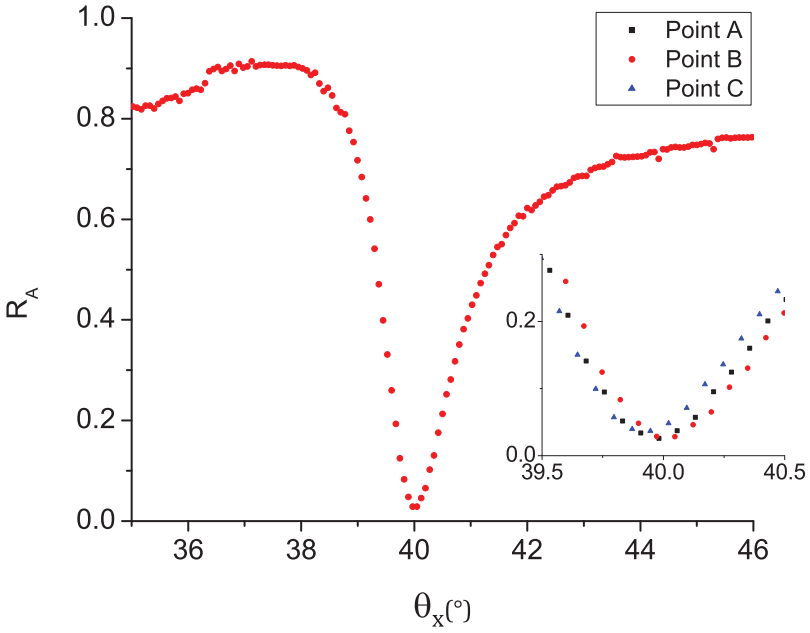

Figure V.4: Typical SPR curve for a gold deposition. The inserted figure represents the SPR curves, close to the ressonance angle, relative to three different points (A,B,C) on the same sample..

In figure V.5 is shown the procedure of fit performed by *Winspall* on the experimental points relative to the region C of the sample under analysis. The corresponding results are listed in table V.3.

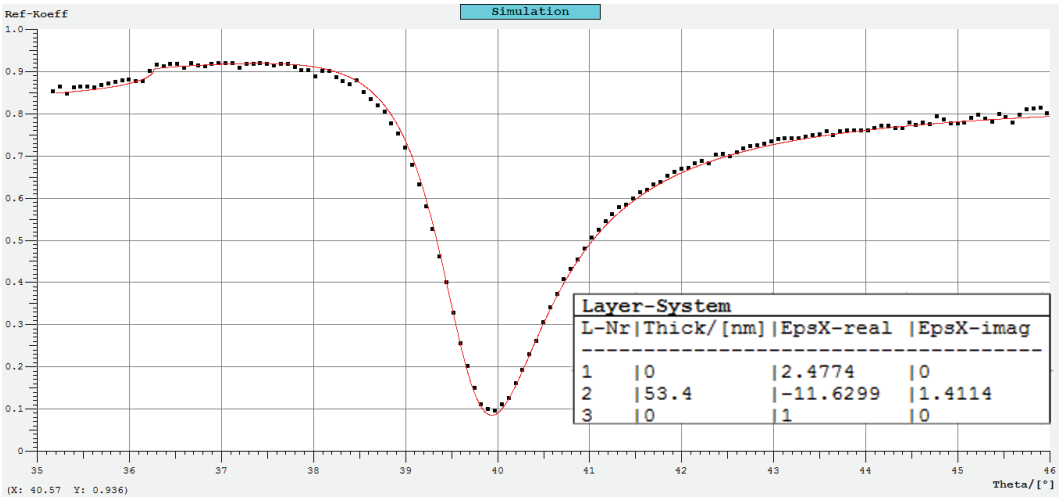

Figure V.5: Fit of the experimental SPR curve obtained with *Winspall* for one point over one of the gold thin films deposited. The black points represent the experimental measurements while the red curve is the theoretical best-fit.

	Thickness (nm)	ε_r	ε_{im}	θ_{SPR} (°)
Mean	52.3	-11.64	1.43	39.947
$\sigma \pm$	0.3	0.06	0.07	0.016
% **Error**	0.6	0.6	5	x

Table V.3: Values obtained for thickness and dielectric function of one of the gold thin films fabricated. The uncertainty of the values reflects the non homogeneity of the metal deposition.

The FWHM of the SPR curve is 1.9°, quite bigger than the one characteristic of silver films. This phenomenon is well known and is due to the higher value of the imaginary part of the dielectric constant of gold in comparison with silver [Hecht06]. The values obtained for the optical constants of gold are similar to the ones reported in the literature [Rueda09, Peter96].
The height profile of the gold layer measured by the profilometer is displayed in figure V.6 The average height thus obtained was (520± 30)Å, very close to the one obtained by SPR spectroscopy.

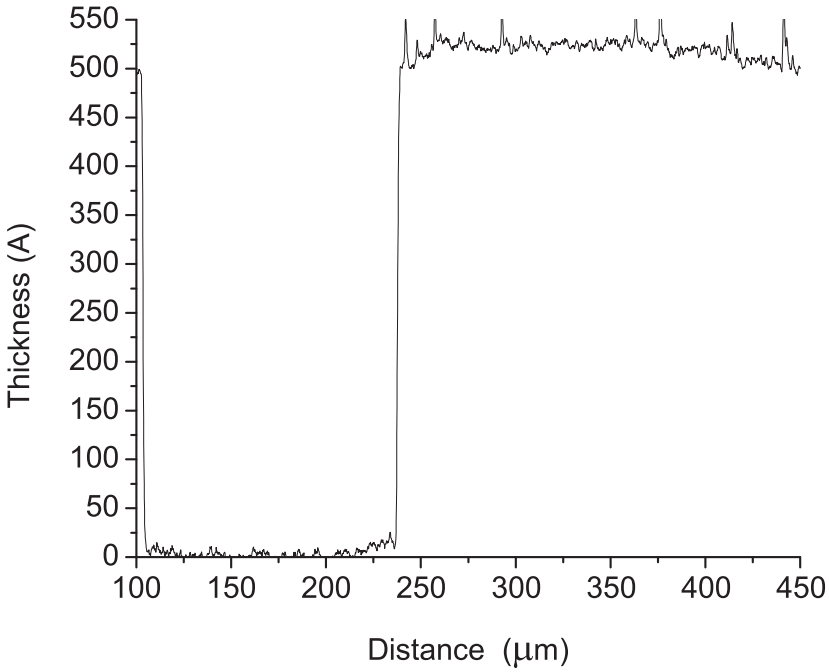

Figure V.6: One of the height profiles relative to the sample with the thin deposition of gold. The height profile has been obtained using the profilometer with a stylus force of 3 mg and a scan length of 400 μm.

The procedure described above was applied to the other samples with gold depositions. The results are presented in table V.4.

Sample	**Thickness** (nm)	$\varepsilon_{\mathbf{r}}$	$\varepsilon_{\mathbf{im}}$	$\theta_{\mathbf{SPR}}$ (°)
1	52.3	-11.64	1.43	39.94
2	54	-11.69	1.44	39.95
3	53.3	-11.70	1.41	39.97

Table V.4: Values obtained for the dielectric function and thickness of different gold thin films fabricated during the same deposition by e-Beam gun apparatus.

It is interesting to note that the dispersion of the optical constants of the different gold films is the same than the one obtained considering the non homogeneity of the gold deposition over one single sample. This fact supports our thesis about the dispersion of the results obtained for the samples with the depositions of silver.

V.3 Measurement of the refractive index of Alq_3 thin film by two-Metal substrate method

A two metal substrate was prepared, half covered by silver and half covered by gold. The metals depositions were followed by a thermal evaporation of 22 nm (nominal thickness = $d_{nominal}$) of Alq_3 in the central part of the sample (pressure = 3.4×10^{-5} Torr, deposition rate = 1.3 Å/s). Finally, the sample was encapsulated following the technique described in III.3.
To start, we performed two independent measurements on the part of the sample covered by the metals without the deposition of the organic material. The results obtained for the optical constants and thickness of the metal depositions are listed in table V.5.

Gold				
	Thickness (nm)	ε_r	ε_{im}	θ_{SPR} (°)
Mean	48.6	-11.76	1.570	39.874
σ ±	0.3	0.06	0.07	0.022
% error	0.6	0.51	4.5	x
Silver				
Mean	45.3	-17.24	0.70	38.564
σ ±	0.3	0.06	0.02	0.022
% error	0.6	0.35	2.86	x

Table V.5: Results obtained for the characterization of the gold and silver films deposited on the sample under analysis.

The SPR curves obtained from the region with the deposition of Alq_3 are shown in figure V.7. The curve with black filled circles is relative to the region with silver and Alq_3 while the curve with open circles is relative to the part of the sample with gold and Alq_3.

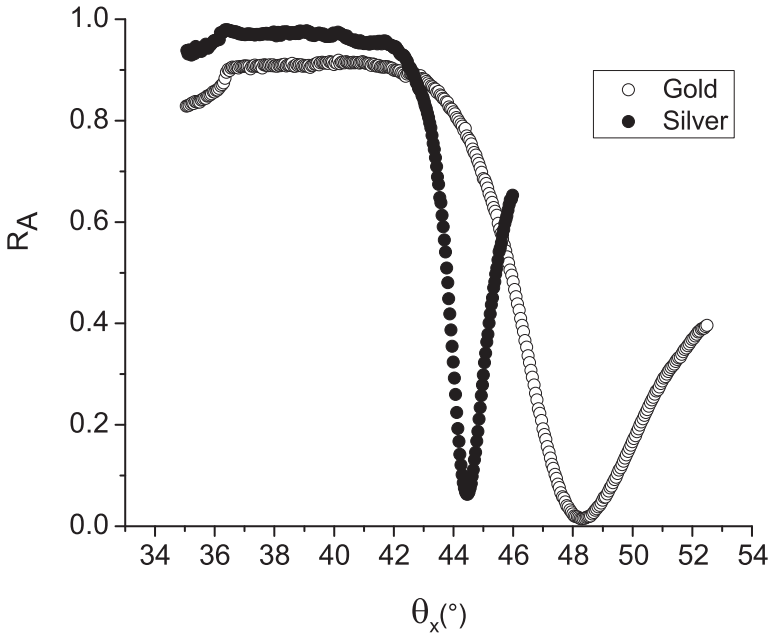

Figure V.7: SPR curves of silver/Aq_3 (black filled circles) and gold/Alq_3 (open circles) samples.

As explained in the first chapter of the thesis, each one of the SPR curves of figure V.7 can be representative of different couples of values of the thickness (d_{Alq_3}) and dielectric constant (ε_{Alq_3}) of the thin organic film. For each one of the multilayer structure (gold/Alq_3, silver/Alq_3) can be generated a continuous curve with the possible solutions in the plane (d_{Alq_3}, ε_{Alq_3}), and the intersection of the two curves represents the actual couple of values that characterizes the thin film of Alq_3. The procedure we used to compute the possible solution of values for each system is the following:

1. First we insert in *Winspall* the value of the thickness and complex refractive measured for the metal film (i.e silver) below the organic material.

2. We insert a guess value for the thickness of the organic thin film (d_{GUESS}).

3. We let *Winspall* performing an iterative procedure to find the value of the dielectric constant of the organic material that together with d_{GUESS} is associated to the theoretical SPR curve that best fits the experimental data. The fit procedure is made considering only a portion of the curve around the experimental angle of resonance θ_{SPR}, namely $\theta_{SPR} \pm 1°$.

4. The same procedure is applied to the multilayer structure with a different metal deposition (i.e gold).

5. We look for the intersection point between the curves $(d_{Alq_3}, \varepsilon_{Alq_3})_{Silver}$ and $(d_{Alq_3}, \varepsilon_{Alq_3})_{Gold}$.

6. The solution found is accepted only if the correspondent value of thickness lies in the region delimited by $(d_{nominal} + 10\%)$ and $(d_{nominal} - 10\%)$, where $d_{nominal}$ is the nominal thickness of the organic layer as read by the crystal balance during the evaporation process and 10% represents the uncertainty we have on the correct value of the Tooling Factor of the deposition.

7. The whole procedure is repeated changing the value of the real part of the dielectric constants of the metal within the limits ruled by the experimental uncertainty $(\sigma\pm)$ of the values reported in table V.5.

An example of simultaneous determination of dielectric constant and thickness of the Alq_3 layer using Two-Metal Substrate Method is shown in figure V.8. The intersection point is located at $d_{Alq_3} = 22.5$ nm and $\varepsilon_{Alq_3} = 3.02$ and the mean values of table V.5 are considered as the dielectric constants of the different metals depositions.

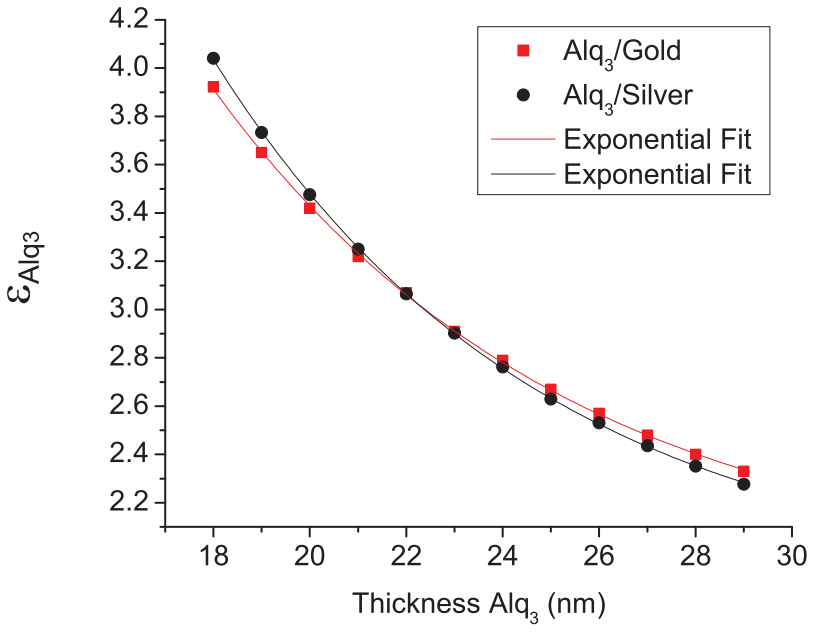

Figure V.8: Curves representing the possible couple of values for the dielectric constants and thickness of the Alq_3 film over silver (black filled circles) and gold (red filled squares) depositions. The mean values of table V.5 are considered as the dielectric constants of the different metals depositions, namely $\varepsilon_{Silver} = (-17,24 + i0,70)$ and $\varepsilon_{Gold} = (-11,76 + i1,57)$.

Figure V.9 shows the intersection points considering different values of the dielectric function of silver and gold within the limits dictated by the experimental uncertainty on their measurement. The final results we obtain for the refractive index and thickness of the Alq_3 layer are

$$d_{Alq_3} = 22.20[20.35; 23.40]nm \qquad n_{Alq_3} = 1.74[1.68; 1.82] \qquad (1)$$

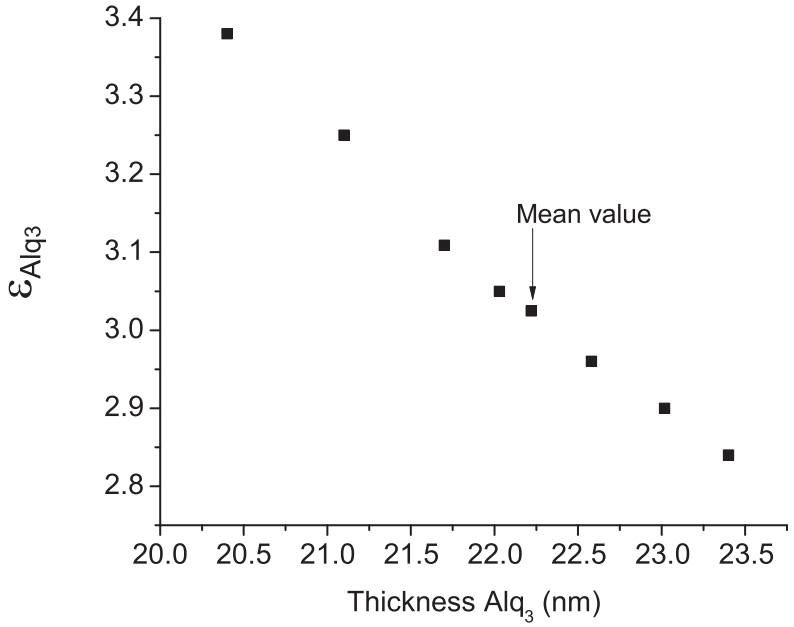

Figure V.9: Possible couples of values for the dielectric function and thickness of the Alq_3 thin film.

Although we used a numerical approach to determine the curves of figure V.8, we could have considered an analytical approach using equation (42) or similar equations developed by Pockrand [Pockrand78]. These equations give very accurate results only in the limit $|dk_z| \ll 1$, that is when the thickness of the material is quite smaller than the penetration of the electromagnetic fields inside the dielectric side of the structure. We developed a program in Mathematica 8.0 language (see Appendix B) to obtain an analytical solution to the problem using equations reported in [Pockrand78]. The results are not very different to the ones we obtained using the numerical approach, with the lower possible value for the dielectric constant of Alq_3 being about 3.10 instead of 2.85 (see figure V.9). The difference between the results obtained with the numerical and the analytical approaches demonstrates that for thickness of the organic material of the order of tens of nm the numerical calculus is to prefer to the faster analytical approach if very accurate results are desired.

V.4 Monitoring of the degradation process of the $gold/Alq_3$ interface

Two gold films with a nominal thickness of 50 nm were deposited on glass slides using the e-Beam apparatus (pressure = 1.9×10^{-6} Torr, deposition rate = 2.3 Å/s), followed by a thermal evaporation of 24 nm of Alq_3 (pressure = 2.4×10^{-5} Torr, deposition rate = 1.3 Å/s). One of the samples has been encapsulated using the technique described in the second chapter of the thesis and the other has been exposed to atmospheric environment. Both of the samples have been monitored for about 2 days by SPR spectroscopy. Figure V.10 represents the behavior of the SPR curve with time for the encapsulated sample. The time interval between each measurement was about 12 hours.

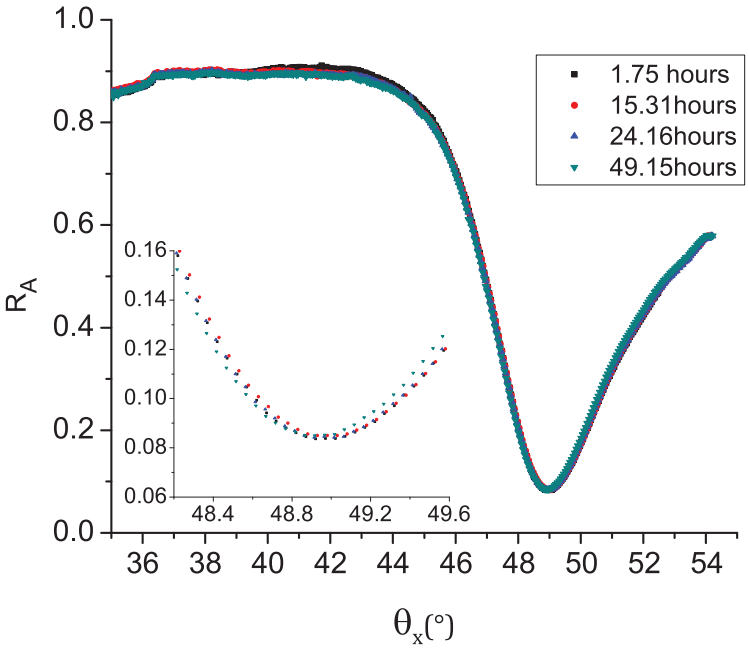

Figure V.10: Behavior of the SPR curve with time for the encapsulated Au/Alq_3 sample. The window at the left-bottom side of the figure is an enlarged view of the SPR curves near the angle of resonance.

The magnitude of reflectivity at the resonance angle does not change with time and the small variation in the position of resonance angle (0.07°), possibly due to temperature fluctuations, is of the same order of the step (30) chosen for measurement. The FWHM of the SPR curve is constant with time, which indicates that there is no alteration in the imaginary part of the dielectric function of Alq_3 or in the morphology of the $gold/Alq_3$ interface.

Also in the case of the non-encapsulated sample, measurements were carried out during about 50 hours. The behavior of the SPR curve of the non

encapsulated sample with time is shown in figure V.11

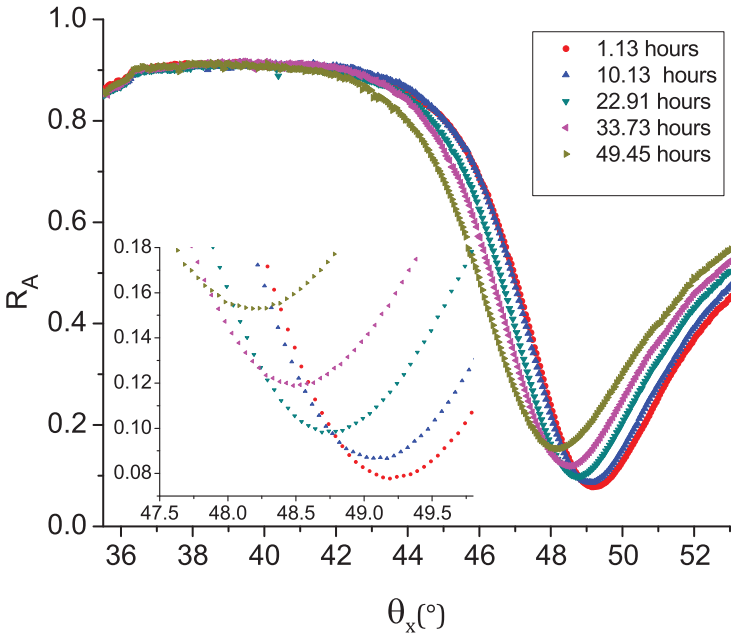

Figure V.11: Behavior of the SPR curve with time for the non encapsulated Au/Alq_3 sample. The window at the left-bottom side of the figure is an enlarged view of the SPR curves near the angle of resonance.

In this case the shape of the SPR curve drastically changes in time with two predominant effects: a huge decrease in the resonance angle θ_{SPR} and an increase of the FWHM of the curve together with the minimum value of the reflectivity. In figure V.12 are represented the behavior of the minimum value of the reflectivity and the resonance angle θ_{SPR} with time. During two days of observation the minimum of the reflectivity passes from 8% to 16% while the angle of plasmon resonance decreases from 49.2° to 48.2°. The results are discussed in the next and last chapter.

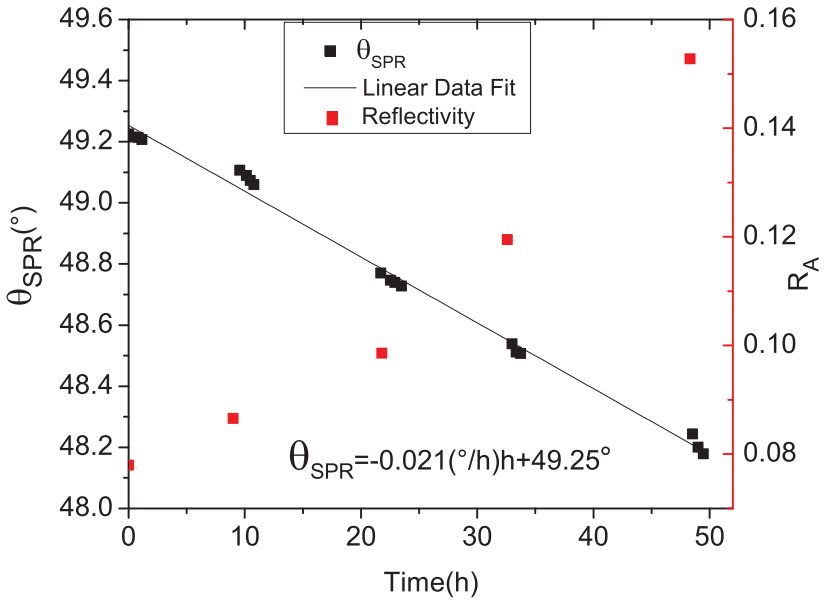

Figure V.12: Time dependence of the minimum value of the reflectivity (right side) and the resonance angle θ_{SPR} (left side) for the non encapsulated Au/Alq_3 sample.